# Relationships between radiation, wildfire and the soil microbial communities in the Chornobyl Exclusion Zone

Alexandre Barretto de Menezes [a],[*], Sergii Gashchak [b], Michael D. Wood [c], Nicholas A. Beresford [c],[d]

[a] University of Galway, School of Biological and Chemical Sciences, Ryan Institute, University Road, H91 TK33, Galway, Ireland
[b] Chornobyl Center for Nuclear Safety, Radioactive Waste & Radioecology, International Radioecology Laboratory, Slavutych, Kyiv Region, Ukraine
[c] School of Science, Engineering & Environment, University of Salford, Manchester M5 4WT, United Kingdom
[d] Centre for Ecology & Hydrology, CEH Lancaster, Lancaster Environment Centre, Library Av., Bailrigg, Lancaster LA1 4AP, United Kingdom

## HIGHLIGHTS

- The impact of radiation contamination in complex ecosystems is poorly understood.
- The soil microbiome in Chornobyl's Red Forest region was sequenced.
- Effect of radiation compared to soil properties, wildfire, and site properties
- Radiation had a minor effect on the soil microbiome.
- Red Forest soil microbiome appears adapted/resistant to current radiation levels.

## GRAPHICAL ABSTRACT
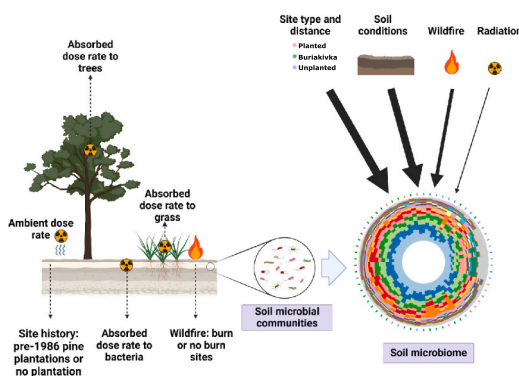


## ARTICLE INFO

## ABSTRACT

There is considerable uncertainty regarding radiation's effects on biodiversity in natural complex ecosystems typically subjected to multiple environmental disturbances and stresses. In this study we characterised the relationships between soil microbial communities and estimated total absorbed dose rates to bacteria, grassy vegetation and trees in the Red Forest region of the Chornobyl Exclusion Zone. Samples were taken from sites of contrasting ecological histories and along burn and no burn areas following a wildfire. Estimated total absorbed dose rates to bacteria reached levels one order of magnitude higher than those known to affect bacteria in laboratory studies. Sites with harsher ecological conditions, notably acidic pH and low soil moisture, tended to have higher radiation contamination levels. No relationship between the effects of fire and radiation were observed. Microbial groups that correlated with high radiation sites were mostly classified to taxa associated with high environmental stress habitats or stress resistance traits. Distance-based linear models and co-occurrence analysis revealed that the effects of radiation on the soil microbiome were minimal. Hence, the association between high radiation sites and specific microbial groups is more likely a result of the harsher

* Corresponding author.
  *E-mail addresses:* alexandre.demenezes@universityofgalway.ie (A.B. de Menezes), sgaschak@chornobyl.net (S. Gashchak), m.d.wood@salford.ac.uk (M.D. Wood).

ecological conditions in these sites, rather than due to radiation itself. In this study, we provide a starting point for understanding the relationship between soil microbial communities and estimated total absorbed radiation dose rates to different components of an ecosystem highly contaminated with radiation. Our results suggest that soil microbiomes adapted to natural soil conditions are more likely to be resistant to ionising radiation than expected from laboratory studies, which demonstrates the importance of assessing the impact of ionising radiation on soil microbial communities under field conditions.

## 1. Introduction

The explosion of reactor 4 at the Chornobyl Power Plant (ChNPP) in 1986 is one of the most notorious examples of an ecological disturbance in recent history, providing an ideal testbed to study how ecosystems adapt to chronic radiation contamination (Mothersill et al., 2022). The explosion led to the largest accidental release of radioactivity to the environment to date (Kuchma and Finkeldey, 2011) and an area of 145,000 km$^2$ of Ukraine, Russia and Belarus was contaminated with caesium-137 ($^{137}$Cs) in excess of 37 kBq m-2 (International Atomic Energy Agency, 2006). An area of approximately 4800 km$^2$ surrounding the Chornobyl power plant was abandoned in 1986 to create the 'Chornobyl Exclusion Zone' (CEZ) (Beresford et al., 2021). Despite a substantial decrease in radiation levels since the accident (the release included many short-lived radionuclides and more than one half-life of $^{137}$Cs has already passed), soils and aquatic sediments in some areas of the CEZ remain highly contaminated with radionuclides (Alexakhin et al., 2007). Consequently, in some areas of the CEZ, organisms, including soil microbial communities, have been exposed to high ionising radiation levels since the nuclear accident in 1986. Considerable research effort has been devoted to study how the local biota responded to the disaster and the impact of chronic radionuclide contamination (Lecomte-Pradines et al., 2020). However, there is still uncertainty regarding the impact of radionuclide contamination on environmental and host-associated microbial communities and ecological processes in the CEZ. While microorganisms are relatively resistant to radiation (McNamara et al., 2007) radionuclide contamination may affect microbial metabolism, particularly the integrity of their proteome and nucleic acids (Jung et al., 2017). Previous studies have detected possible links between soil radiation contamination in the CEZ and shifts in radioactive waste trench soil microbial community composition (Theodorakopoulos et al., 2017), and functional gene pools (Hoyos-Hernandez et al., 2019). Microbial communities in CEZ wetlands, including soils, have also been found to be impacted by radiation (Videvall et al., 2022). Contrasting relationships between soil radiation contamination and organic matter decomposition have been reported (Bonzom et al., 2016; Mousseau et al., 2014) and ionising radiation doses as determined in 2016 have been reported to not directly impact on soil (invertebrate) biological activity in the CEZ (Beresford et al., 2022). Furthermore, while the gut microbiome of earthworms in the CEZ were found to correlate with dose rate, this correlation was considered to be linked to co-variation between soil properties (especially pH) and dose rate and consequently it was not possible to attribute microbiome changes to radiation exposure (Newbold et al., 2019). Similarly, although some studies have reported responses in bank vole (*Myodes glareolus*) gut microbiome to radiation in the CEZ (Lavrinienko et al., 2020, 2018), a further study recently showed that correlations between radiation dose rate and bank vole gut microbiome were not robust against variations in habitat and geographical location in the CEZ (Antwis et al., 2021). Interestingly, radiation affected the gut microbiome of three ground-dwelling *Apodemus* mice species in the CEZ and the Fukushima Exclusion Zone (FEZ), but not that of a tree-dwelling species in the FEZ (Lavrinienko et al., 2021).

There is increased focus on using an ecosystem approach to evaluate the impact of radiation on biodiversity to support radiation protection (Mothersill et al., 2022). However, many studies focus on quantifying the effects of radiation at the molecular level, such as increased

mutation rates, changes in gene expression and DNA damage, which may have only slight effects at the population level (Boubriak et al., 2016; Geras'kin et al., 2013). For example, chronic radiation caused oxidative stress in Scots pines near Chornobyl, but had no impact on their enzyme activities (Volkova et al., 2017), while annual ring thickness data suggested that pines that were exposed to sub-lethal radiation in 1986 showed little evidence of ongoing radiation damage (D. Holiaka et al., 2020). At the same time, the effect of radiation on organisms assessed under field conditions can be related to the presence of additional stresses that affect the survival of organisms in contaminated environments (Mothersill et al., 2022). This is compounded by the difficulty of obtaining robust field data from radiation-contaminated environments, where variation in exposure influences the overall effect of radiation on biodiversity (Mothersill et al., 2022; Stark et al., 2017). For effective biodiversity radiation protection measures, it is important to understand the effects of radiation in natural, complex ecosystems and take into account other environmental variables that may also impact biodiversity, including site history (Mothersill et al., 2022).

Understanding how radiation affects microorganisms in the natural environment is also made difficult by the fact that radiation resistance is linked to resistance to other environmental stresses (Jung et al., 2017). Ionising radiation damages both the cell's proteome and genome and generates DNA double-stranded breaks (DSBs) which can be lethal to microorganisms (Shuryak, 2019). Key mechanisms of radiation resistance are associated with detoxification of reactive oxygen species (ROS) and mechanisms that repair DSBs (Daly, 2023). The accumulation of antioxidant manganous (Mn$^{2+}$) complexes that protects the proteome has been found to be one of the best predictors of resistance to ionising radiation, likely because it allows the preservation of the cells' enzymes involved in DNA damage repair (Sharma et al., 2017). As many microbes can withstand ionising radiation doses vastly superior to levels in their natural environment, it has been hypothesized that ionising radiation resistance mechanisms evolved as a response to other stressors, e.g. UV light and desiccation among others (Sharma et al., 2017). As with ionising radiation, desiccation leads to oxidative stress that damages both the genome and the proteome, while radiation resistance and desiccation resistance are correlated across the tree of life (Daly, 2023).

In July 2016 a wildfire affected approximately 80 % of the 'Red Forest', the most contaminated terrestrial ecosystem within the CEZ (Beresford et al., 2021). The Red Forest is an area of approximately 4–6 km$^2$ to the west of the Chornobyl Nuclear complex where pine trees were killed by high levels of radiation in 1986. Wildfires represent a major disturbance to forests, and their ecological impacts depend on the interactions between fire intensity, frequency, type, severity and size (Flannigan et al., 2009). Forest fires can have considerable direct and indirect effects on the belowground ecosystem, with intense fires killing most microbial life in the top layers of soil (Dooley and Treseder, 2012), and subsequent shifts in microbial community composition (Cobo-Díaz et al., 2015; Prendergast-Miller et al., 2017). Fires can also have long-lived impacts in the soil by changing the soil organic matter quality, pH, moisture retention capacity, buffering capacity and nutrient availability (Prendergast-Miller et al., 2017).

In this study, we investigated the soil microbiome in the Chornobyl Exclusion Zone, largely within the Red Forest (additional sampling sites were in deciduous woodlands approximately 8 km to the west of the Red Forest near the village of Buriakivka), along gradients of soil radiation contamination, and from burn and no burn sites following the 2016 Red

Forest fire (Fig. 1). Further, our study sites within the Red Forest were distributed along two distinct land-use histories corresponding to areas which had or had never been planted with conifers prior to the 1986 explosion. The soils in areas of the Red Forest that had been planted with pines (termed 'Planted' sites in this paper) were also characterised by generally higher radionuclide contamination levels compared to those sites that had never been planted with conifers (termed 'Unplanted' sites). The Unplanted sites within the area considered here as the Red Forest were either in established deciduous woodland or forest clearings. We used distance-based linear modelling (DistLM) to determine the importance of spatial distance, site type (Buriakivka, Planted and Unplanted), burn, soil properties (soil pH, moisture, soil nitrate and ammonium, and grass, other vegetation and total vegetation dry mass) and radiation (ambient dose rates as well as total absorbed dose rates for grassy vegetation, bacteria and trees) in determining the soil microbial community structure. Co-occurrence network analysis was used to determine the presence of microbial network modules and the relationships between the modules and radiation, as well as to investigate correlations between individual microbial taxa and radiation.

## 2. Methods

### 2.1. Soil collection

Soils were collected in September 2017 from 20 sites of varying radiation, soil quality and burn score levels in the Red Forest and from three reference sites (referred to as Buriakivka) located outside of the Red Forest, but in an area of the CEZ with soil radionuclide contamination that is still notably higher than most soils globally and a vegetation cover similar to that of the Red Forest (Fig. 1). At each site, there were $3 \times 1\ m^2$ plots within 30 m of each other. The majority of the study plots had previously been used in a study of soil biological activity in spring 2016 prior to the Red Forest wildfire, and the plots were re-established after the forest fire and new ones added in September 2016 (Beresford et al., 2022). As they were established only two months after the wildfire it was possible to determine if the plot had been impacted by the fire. Plots were scored objectively by two of the authors as: 1 - no area of the plot burnt (termed 'No Burn' samples); 2 - some or all areas of plot burnt ('Burn' samples). Plot locations were recorded using a GPS (accuracy approximately 3 m) and ambient dose rate (µSv h$^{-1}$) on the soil surface was measured at each plot using a beta-shielded MKS-01R dosimeter. In September 2017, five surface (10 cm deep) soils were collected from each plot using a 2.5 cm diameter soil corer after removal of surface leaf litter, composited and transferred to a field station located in Chornobyl town for processing. Soils were 2 mm sieved and aliquots were taken for nutrient analysis and DNA extraction. Soils were kept cold at 4 °C for a maximum of 3 days before processing for soil nutrient and DNA extractions. Soil biological activity was determined using the bait lamina method, which measures soil organism feeding activity in situ as described in a previous study (Beresford et al., 2022).

### 2.2. Soil analyses

Soil subsamples were extracted with 1 M KCl (1:4 *w/v* ratio). Extracts were analysed for N pools: ammonium ($NH_4^+$) and nitrate ($NO_3^-$) using a microplate reader (SynergyMX, BioTek; Winooski, VT). Soil nitrogen
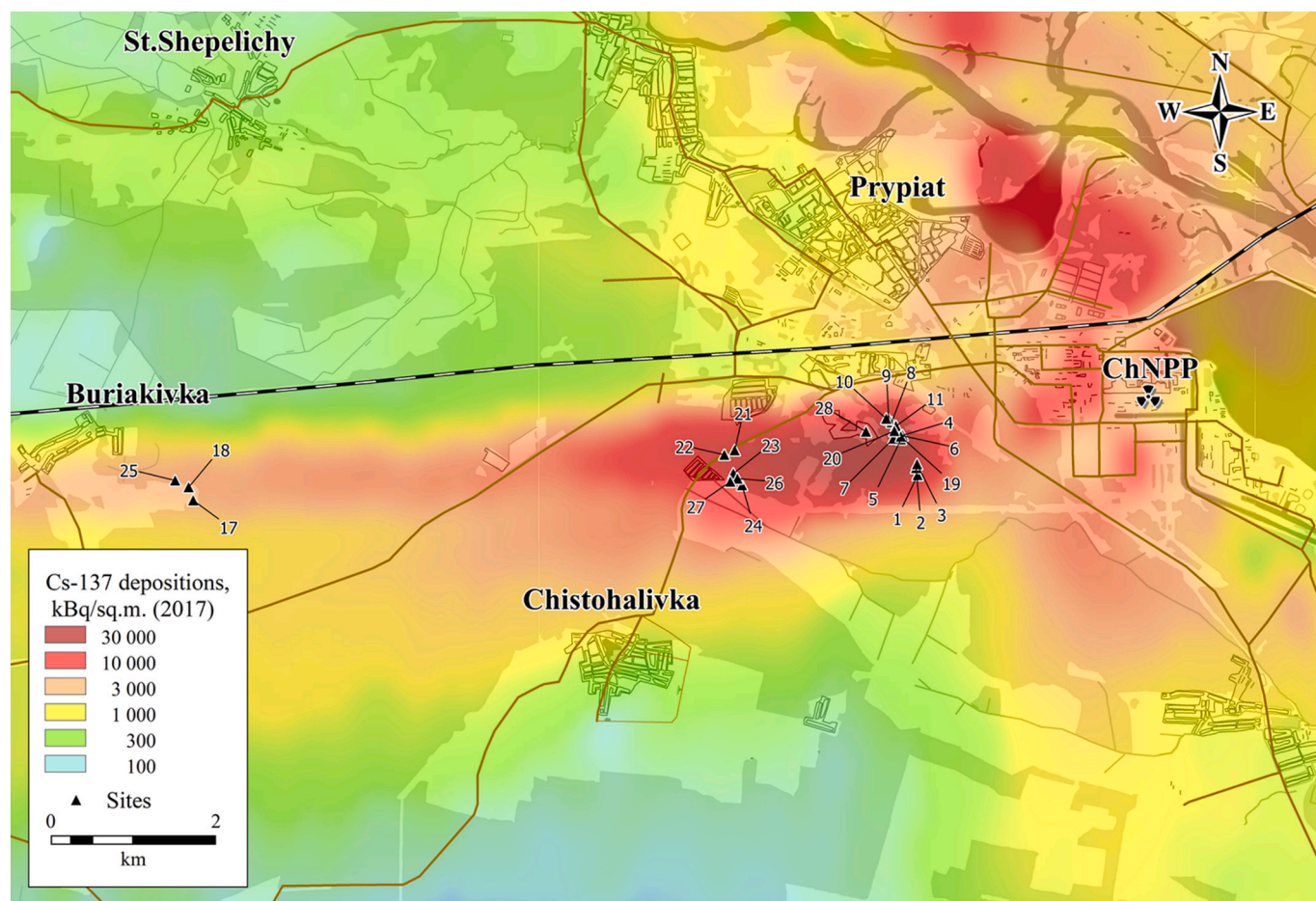


**Fig. 1.** Map of the study area in the Chornobyl Exclusion Zone (CEZ), showing sampling sites. Planted sites: 4, 5, 6, 7, 8, 9, 10, 11, 19, 20, 21; Unplanted sites: 1, 2, 3, 22, 23, 24, 26, 27, 28. Sites 17, 18, 25 are the reference sites (Buriakivka). ChNPP = Chornobyl Nuclear Power Plant.

pools are expressed on a soil dry mass basis. Soil pH was measured using a 1:5 w/v in water and soil moisture was determined gravimetrically after drying at 65 °C overnight. Soil loss-on-ignition (LOI) (total organic matter content) was estimated using the methodology of Allen (Allen, 1974). Caesium-137 ($^{137}$Cs), americium-241 ($^{241}$Am), strontium-90 ($^{90}$Sr) and plutonium-238,239,240 (Pu-isotopes) activity concentrations in soils were determined by the Chornobyl Center using methodology detailed elsewhere (Barnett et al., 2021) and can be accessed here https://catalogue.ceh.ac.uk/documents/60782622-7bfa-461 5-a9e3-0a802a9f4674.

### 2.3. Vegetation analyses

All above ground vegetation was collected from each 1 m$^2$ plot at the same time as soils were sampled. In the Chornobyl laboratory the vegetation samples were separated into 'grassy' (grass and sedge species) and 'other' (e.g. herbaceous and woody species) vegetation, dried at 20–25 °C and the dry mass (DM) recorded. $^{137}$Cs and $^{90}$Sr activity concentrations in samples were determined using the methods described in Barnett et al. (2021).

### 2.4. DNA extraction and sequencing

Soil samples (0.25 g) from 69 samples (one for each composite soil samples from the 1 m$^2$ plots) in addition to three blank controls (distilled water) were added to bead-beating tubes containing glass beads and 1 ml DNA/RNA shield (Zymo Research), and DNA extracted by bead-beating using super-fast prep homogenizer (Mpbio). The extracts were spun in a bench-top centrifuge and supernatant collected, frozen, and transported to the University of Galway where DNA extraction was completed. The presence of contaminant humic compounds and proteins in DNA extracts were determined using NanoDrop™ and DNA was quantified using Quanti-iTTM Picogreen (Life Technologies) and sent for sequencing using the Illumina MiSeq platform at the Centre for Genomics Centre – University of Liverpool. A mock bacterial community (Zymo research) and a negative control was included in the sequencing project. Following quantification using QubitTM (Life Technologies), the V4 variable regions of the bacterial 16S rRNA gene was amplified using the 515f and 806r bacterial 16 s rRNA primers (254 bp insert size) (Caporaso et al., 2011), which were adapted to contain barcodes and the Illumina linker sequence, and equimolar amounts of DNA were added to one MiSeq flow cell. Sequencing was carried out in an Illumina MiSeq sequencer using a V2 sequencing kit (paired-end, 2 × 250).

### 2.5. Microbiome DNA sequence processing

Sequence quality was evaluated using FastQC to determine sequence quality filtering parameters. Barcodes and adapters were removed using Flexbar version 3.4.0 (Roehr et al., 2017). Using the DADA2 R package, filtered sequences were truncated at 210 (R1) and 200 (R2) base pairs (truncLen = c(210,200)), maximum expected errors was set to 3 (maxEE = 3), quality score to 11 (truncQ = 11), and no ambiguous bases (maxN = 0). 16S rRNA gene sequences were subject to mate-pair merging, chimera removal, and biological sequence variant determination following the microbiome sequence analysis pipeline described in Callahan et al. (2016). Amplicon sequence variants (ASVs) were classified using the assignTaxonomy DADA2 command based on the curated Silva database, version 138.1 (Quast et al., 2012). A total of 168 ASVs detected in the three extraction control samples were removed from the dataset. Sequences classified as eukaryotic, chloroplast, mitochondria, and those not classified to kingdom level, were removed from the dataset. Sequences were aligned using MAFFT (strategy FFT-large-NS-2) and aligned using FastTree using the Jukes-Cantor model of DNA substitution. Three samples were removed from the dataset due to low numbers of sequences (53–2873 sequences), and the final dataset had 66 samples with 93,519–288,959 sequences, with 32 samples from Planted

sites, 25 from Unplanted sites and 9 from Buriakivka. There were 11 No Burn samples (6 and 5 from Planted and Unplanted respectively) in the Red Forest, while all Buriakivka samples were No Burn. There were 46 Burn samples (26 and 20 from Planted and Unplanted respectively). The raw 16S rRNA sequences were deposited in the European Bioinformatic Institute (https://www.ebi.ac.uk/metagenomics/), with study name PRJEB50900.

### 2.6. Estimating organism dose rate

The ERICA Tool (version 1.3) (Brown et al., 2016, 2008) was used to estimate indicative weighted absorbed dose rates (μGy h$^{-1}$) to grassy vegetation and deciduous trees (the dominant tree type across all sites where trees were present) at each study plot. For the estimation of ambient external dose rate, the measured soil activity fresh mass concentrations were used. To determine total dose rate, measured $^{90}$Sr and $^{137}$Cs activity concentrations for grassy vegetation were used together with transfer parameter values determined for *Agrostis gigantea* from a site within the Red Forest (Beresford et al., 2020a) to estimate $^{241}$Am and Pu-isotope activity concentrations in grassy vegetation. To determine $^{90}$Sr and $^{137}$Cs activity concentrations in deciduous trees transfer parameter values determined at sites within the CEZ were used (D.M. Holiaka et al., 2020) together with $^{241}$Am and Pu-isotopes transfer parameter values for *Pinus sylvestris* (wood) from a site within the Red Forest (Beresford et al., 2020a). The ERICA Tool version 1.3 did not allow dose rates to soil bacteria to be estimated, so the revised 'R&D128' spreadsheet model (Copplestone et al., 2001) (available from https://wiki.ceh.ac.uk/display/rpemain/Ar+-+Kr+-+Xe+dose+calculator) was used; for the radionuclides of interest and similar organism geometries the two models are known to give similar dose estimates (Vives I Batlle et al., 2011, 2007). Radiation weighting factors of 10 for alpha emissions, 3 for low energy beta and 1 for other beta and gamma were used. Note grassy vegetation absorbed dose rates were only estimated for those plots (n = 55) from which grassy vegetation was sampled (termed grass cover samples in this study); total absorbed dose rates were estimated for bacteria and trees at all plots (though in reality a few plots did not have trees present). For simplicity, ambient dose rate is shortened as ADR and grassy vegetation, bacteria and tree total absorbed dose rates are shortened as GDR, BDR and TDR, respectively.

### 2.7. Statistical analyses

Analyses of microbial beta-diversity were carried out following the filtering of ASVs that: a) did not occur in at least 2 % of samples or b) which had <10 sequences overall, resulting in a total of 26,708 ASVs in the filtered ASV table. This filtering of low frequency ASVs was carried out as low abundance, infrequent microbial taxa have a greater probability of representing sequencing errors (Rosen et al., 2013), and a filtering approach used previously (de Menezes et al., 2018) was applied here. To evaluate how results may differ when the microbial data is processed using alternative strategies commonly used in microbiome research, we calculated a) an Aitchison distance matrix from the ASV abundance table using the dist_calc function from the microViz R package; b) weighted UniFrac distance matrix calculated using the distance command from the phyloseq R package and ancom-bc (Lin and Peddada, 2020) bias corrected ASV data, c) Bray-Curtis distance matrix calculated in PRIMER 7 (Anderson et al., 2008) from medium-normalised ASV data. The different microbial abundance data were used for DistLM, MVDISP and PERMDISP analyses. Grass dose rates could not be calculated for 11 samples (8 in the Red Forest) where there was no grass cover. As result, DistLM was calculated both for the sets of samples which included samples with and without GDR. DistLM was carried out separately for a) Planted, Unplanted and Buriakivka samples together (termed 'All Sites'), b) Planted and Unplanted sites together (Red Forest), and c) Planted and Unplanted sites separately.

For the environmental variables, individual radionuclide soil activity

concentrations were removed from the analyses, as they are used in the calculation of dose rates. Environmental variables (soil pH, moisture, ammonium, nitrate, LOI, vegetation dry mass [grass, total and other vegetation], soil biological activity [number of bites]) were log $(x + 1)$ transformed to reduce skewness in the data. Spatial coordinates were obtained based on latitude and longitude data and were mean-centred using the scale function in R. Differences in soil property and dose rates between site types (Buriakivka, Planted and Unplanted), Burn and No Burn were analysed using Kruskal Wallis non-parametric analysis of variance test (Kruskal and Wallis, 1952).

Multivariate dispersion index analysis (MVDISP) was used to determine ß-diversity (community composition heterogeneity) for sample groups (Planted, Unplanted, Burn and No Burn) and PERMDISP was used to test the homogeneity of variance and was carried out using 9999 permutations and including pairwise tests. MVDISP and PERMDISP were calculated using the PRIMER 7 software (Anderson et al., 2008).

Distance-based linear modelling (DistLM) was used to investigate the importance of the environmental variables measured, in particular ambient and estimated total absorbed radiation dose rates, and microbial communities. Except for estimated dose rates, no environmental variable co-correlated with $r > 0.8$, and were all included as starting terms when running DistLM. All estimated dose rates showed correlations >0.8 to each other, while correlations >0.9 were found between bacteria dose rate and ambient dose rate, grass dose rate and ambient dose rate, and bacteria dose rate and tree dose rate. Due to this co-correlation, DistLM was run several times, with only one dose rate run at a time. The xy spatial coordinates were grouped as a set in the DistLM models to allow the determination of the importance of spatial distance on microbial community variation. To determine the contribution of site type (Buriakivka, Planted and Unplanted) and burn status and site history were coded into the DistLM model by assigning a binary value to each condition (e.g. 1 or 0 for Burn and No Burn sites, respectively) (Anderson et al., 2008). DistLM analysis was carried out separately for All Sites (Red Forest and Buriakivka), Red Forest only, and Planted and Unplanted sites separately. In addition, as many samples lacked GDR, it was necessary to repeat the DistLM for the subset of samples for which GDR was available to evaluate the importance of GDR relative to the other estimated total absorbed dose rates. Marginal tests were carried out prior to model building, and variables that were not significant (p value >0.05 after FDR correction) were removed from models. For the final models, only BDR was included to avoid collinearity with other dose rates. Evidence for relationships between the effects of burn and BDR on the soil microbiome was investigated by determining the change in the variability explained by BDR when fitted before and after each significant variable (once all other significant variables were fitted and their variation removed) of the Red Forest DistLM models.

To visualise differences in microbial communities composition between different site types, Burn and No Burn sites, non-metric multidimensional scaling (nMDS) ordination was carried out using the capscale function from the vegan R package (Dixon, 2003). For the nMDS, square root transformed family level microbial abundance and Bray-Curtis distance was used, and environmental variables with a correlation >0.8 between species and axes were plotted as vectors. Microbial alpha diversity indices were determined by calculating the Shannon index (an alpha-diversity index in which richness and evenness are weighted equally), the Simpson index (an alpha-diversity index which gives greater weight to evenness) (Jost, 2006), the Pielou evenness index and richness (total number of ASVs observed) using the diversity function from the vegan R package (Dixon, 2003).

### 2.8. Co-occurrence network analysis

Co-occurrence network analysis was performed using Weighted Gene Correlation Network Analysis (WGCNA) (Langfelder and Horvath, 2008), using samples for which GDR was available (N = 55). Prior to WGCNA analysis, all ASVs that did not occur in at least 30 % of samples

were removed, and the abundance data was Hellinger-transformed and log-scaled, while the sample metadata was log $(x + 1)$ transformed. The WGCNA soft threshold (sft = 8) was identified by raising the power until approximate scale-free topology was obtained and a signed network was built using the adjacency and TOMsimilarity WGCNA commands. The signed network considers only positive associations when building the network. Network modules (groups of ASVs that co-correlate strongly) were detected using average linkage hierarchical clustering which groups ASVs in a hierarchical clustering tree. This was carried out using the cutreeDynamic command with a minimum module size of 30 ASVs. Modules with dissimilarity threshold lower than 0.3 were merged. Subsequently, the relationships between modules and soil variables were analysed by calculating the first principal component of each module (the module eigengene), which summarises ASV abundance profiles within the module, and by correlating the module eigengene with environmental variables. To identify microbial taxa which correlated with dose rates only, the cor function of the WGCNA package was used to correlate (Pearson correlation) the dose rates and soil variables to individual ASVs within the network. Non-significant p-values were removed and the qvalue WGCNA command was used to calculate q-values (Storey, 2002) from the set of p-values generated and estimate the false discovery rate. To select ASVs that correlated with dose rates, only ASVs that had a q-value <0.05 for a dose rate but with q-value >0.05 for non-radiation soil properties were retained.

## 3. Results

Data for soil radionuclide activity concentrations, ambient dose rates, estimated organism absorbed dose rates, vegetation dry masses, basic soil parameters (pH, loss-on-ignition etc.) and site notes (burn, site history etc.) can be found in Barnett et al. (2021).

### 3.1. Soil parameters

Compared to Buriakivka, Planted sites had lower 'other' vegetation dry mass and lower soil biological activity while Unplanted sites had higher total vegetation dry mass. The soils from Planted sites had lower moisture, lower nitrate, lower biological activity and lower 'other' and total vegetation dry masses compared to Unplanted sites ($p < 0.05$) (Table S1A). When comparing soil variables between Burn and No Burn samples, ammonium was higher in the Burn compared to No Burn soils.

### 3.2. Dose rates

Bacterial, grassy vegetation, tree estimated total absorbed dose rates and ambient dose rates were higher at the Red Forest Planted and Unplanted samples than at Buriakivka ($p < 0.05$) (Table S1B). Dose rates were significantly higher in Planted than Unplanted samples, except for TDR, where the difference was not significant. Differences in ADR, BDR, TDR and GDR were not significant between Burn and No Burn (Table S1B). Overall ambient dose rate and estimated bacterial, tree and grass absorbed dose rates varied approximately 17-, 76-, 85-, 29-fold for Planted Red Forest samples, and 7-, 19-, 21-, 6-fold in Unplanted Red Forest samples. Across the study, log-transformed ADR and GDR were correlated ($r = 0.93$), as were BDR and TDR ($r = 0.94$), ADR and BDR ($r = 0.95$), ADR and TDR ($r = 0.88$), GDR and BDR ($r = 0.89$) and GDR and TDR ($r = 0.85$).

### 3.3. Microbial communities

The total number of observed microbial ASVs, Shannon, Pielou and Simpson indices were not significantly different between Planted and Unplanted sites, although there is a trend of lower richness in Planted sites' soils (Fig. 2). Planted had lower Shannon and Pielou indices than Buriakivka. Burn had no statistically significant effect on microbial alpha diversity indices (data not shown).
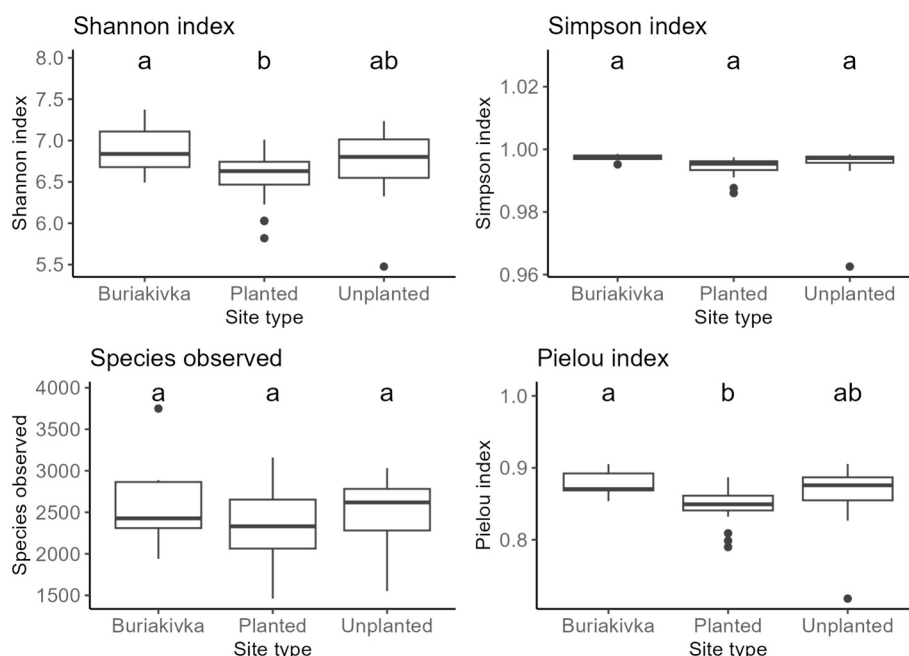
**Fig. 2.** Alpha diversity indices for Buriakivka, Planted and Unplanted sites.

## 3.4. MVDISP results

Multivariate dispersion analysis showed that Unplanted samples were significantly more heterogenous than Planted samples and Buriakivka, regardless of what community distance measure was used (Table 1). Burn samples were more heterogenous than No Burn except when using Aitchison distance, in which case this difference was not significant. Due to the significant differences in dispersion, it was not possible to use PERMANOVA or similar tests to determine the significance of differences in community structure between Planted and Unplanted, or between Burn and No Burn. This is because it is impossible to determine whether significant PERMANOVA results were due only to variations in dispersion, or dispersion and community structure.

## 3.5. Microbial community composition

The classes Planctomycetes, Actinobacteria, Alphaproteobacteria, Acidobacteria, Verrucomicrobia, phylum WPS-2, Gammaproteobacteria, Ktedonobacteria (Choloroflexi), AD3 (Choloroflexi) were the most abundant in most samples (Supplementary Fig. S1). Multidimensional analysis (Fig. 3) showed no clear separation between Planted and Unplanted samples. Planted samples clustered together, while Unplanted samples did not. The Unplanted samples with relatively high radiation contamination grouped with the Planted samples, while Unplanted samples with relatively low radiation contamination were dispersed in the plot, with some clustering with the Planted samples and others

**Table 1**
MVDISP dispersion of microbial community data. Shared letters within the same column represent non-significant PERMDISP p-value.

| Site type | Aitchison distance | Bray-Curtis distance, medium normalised | Ancom-bc bias correction |
|---|---|---|---|
| Buriakivka | 0.986[a] | 0.833[a] | 1.011[a] |
| Planted sites | 0.753[a] | 0.764[a] | 0.785[a] |
| Unplanted sites soil | 1.41 | 1.411 | 1.354 |
| Red Forest No Burn | 0.809[a] | 0.722 | 0.736 |
| Red Forest Burn | 1.035[a] | 1.051 | 1.048 |

forming two distinct outlying clusters. The samples in these outlying Unplanted clusters tended to have high soil moisture, while one of those clusters also had higher soil pH than most other samples (Supplementary Fig. S2A and B). The samples did not cluster based on burn status. One of the outlying clusters of Unplanted samples correlated with Vicinamibacteria (phylum Acidobacteria). The same cluster had comparatively lower abundances of classes Planctomycetes, Actinobacteria and Gammaproteobacteria. The Ktedonobacteriaceae, AD3 and the Gemmataceae correlated with a subset of Red Forest samples along the MDS2 axis, while opposite to this cluster, the families Subgroup 1 of the Acidobacteriaceae, Burkholderiaceae, Pedosphaeraceae, Acidothermataceae, unclassified Acidimicrobia and LWQ8 (Unclassified Bacteria) correlated with a different set of Red Forest samples. The unclassified P_WPS2, Mycobacteriaceae and Isosphaeraceae correlated with Red Forest samples that are intermediate along the MDS2 axis.

## 3.6. DistLM results

DistLM marginal tests carried out with Aitchison distance matrices of 16S rRNA community data (Table 2) showed that dose rates had significant marginal test correlations with soil microbial community structure when analysing All Sites, Red Forest only and Unplanted sites. However, for the Planted sites, dose rates were not correlated to microbial community structure. Final DistLM variable selection for samples with grass cover showed that ADR, BDR and TDR but not GDR were included in the final models for All Sites and Red Forest models while for Unplanted, only ADR were included in the final DistLM model. When including samples without grass cover, BDR and TDR were not included in the final Red Forest models and ADR was not included in the final Unplanted models (Table 2).

The inclusion of dose rates in the final DistLM models was sensitive to the type of distance matrix used. DistLM models for weighted UniFrac distance tended to include dose rates less frequently in the final models, with the opposite being observed for Bray-Curtis distance final models (Supplementary Table S2). However, similar trends as in Aitchison distance models can be observed, with dose rates being included more frequently in the All Sites and Red Forest models than in Planted and Unplanted modes. For the Unplanted sites, ADR was included in final models for weighted UniFrac distance with grass cover samples only,
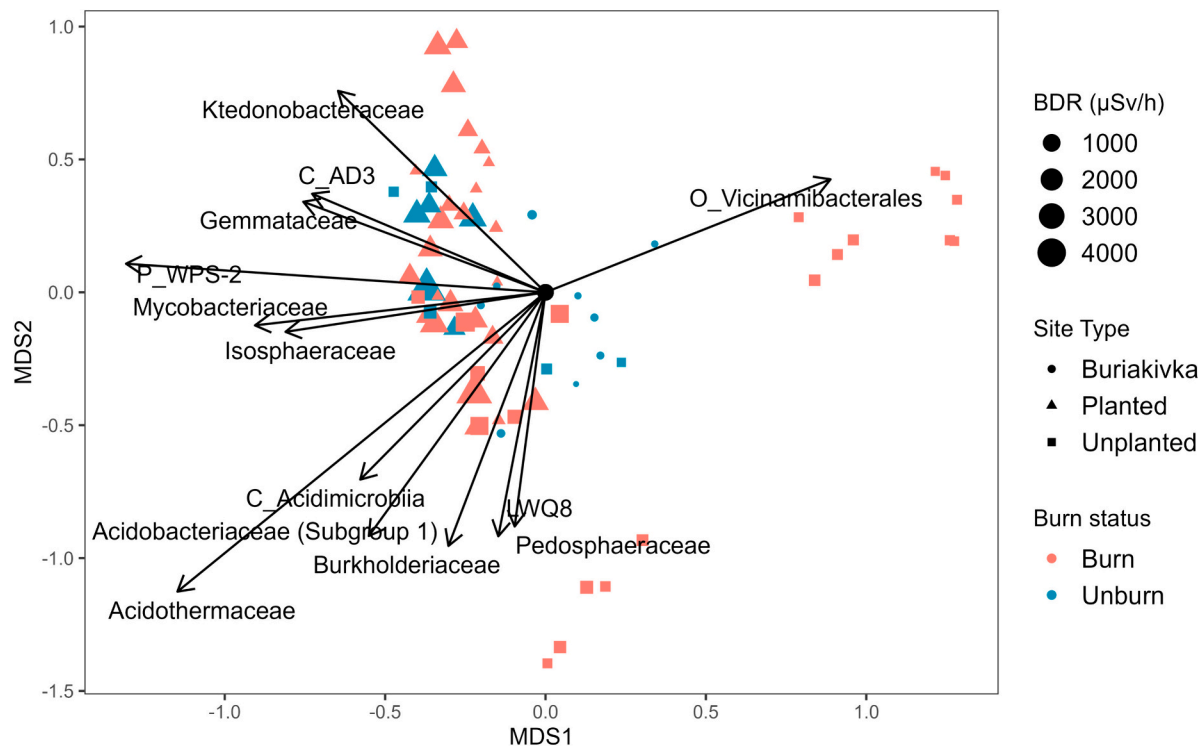
**Fig. 3.** Multi-dimensional scaling (MDS) of prokaryote diversity in Planted samples (triangles), Unplanted samples (squares) Red Forest soils and reference site samples (Buriakivka) (circles). Arrows represent correlations > 0.8 between prokaryote families and MDS axes. Symbol sizes are mapped to estimated total dose rate to bacteria. BDR = total absorbed bacteria dose rate.

**Table 2**
Inclusion of ambient (ADR), grass-absorbed (GDR), bacteria-absorbed (BDR) and tree-absorbed (TDR) dose rates in DistLM models using 16S rRNA gene abundances and Aitchinson distance. Values shown are the p-values of dose rate inclusion in the model obtained with 9999 permutations. Since grass dose rates were not available for all samples, where a dose rate was significant when analysing samples for which grass dose rates were available, these are shown separated by a forward slash (/). NS, non-significant. M, significant in marginal test but not included in DistLM model.

| Aitchison distance | All sites (N = 66/55) | Red Forest (N = 57/49) | Planted (N = 32/30) | Unplanted (25/19) |
|---|---|---|---|---|
| ADR | 0.0117/ 0.024 | 0.0179/0.03 | NS/NS | M/0.0198 |
| GDR | /M | /M | NS | M |
| BDR | 0.0184/ 0.0231 | M/0.0261 | NS/NS | M/M |
| TDR | 0.0323/ 0.0274 | NS/0.0364 | NS/NS | NS/M |

while for the Bray-Curtis distance model ADR was included in the final model when including all samples. In Planted sites' models, no dose rate was significant in marginal tests for both weighted UniFrac and Bray-Curtis distance, and therefore were not included in the final models.

Focusing on Aitchison distance and BDR models built with grass cover samples, the final DistLM models showed that BDR, when included in the models, only explained up to 2.16 % of variation in community composition, while the overall models explained 18.10–52.35 % of total variation (Table 3). This is a similar level of explained variability as observed for $NO_3$ (up to 2.26 %), LOI (up to 2.56 %) and other vegetation dry mass (up to 2.28 %). Site type and spatial distance generally explained considerably more variation in microbial community structure compared to all other variables, while pH was the most important variable for Unplanted sites. Soil moisture was included in all models built while burn was included in all except the Planted sites' model. LOI,

**Table 3**
DistLM models showing variables that best explain variation in microbial community composition. Data used to build model was Aitchinson distance calculated from samples which had grass cover. Only estimated total absorbed dose rate to bacteria (BDR) was included in the models to avoid including colinear variables. GDM = grass dry mass; LOI = loss on ignition; other veg DM = other vegetation dry mass.

| Dose rate | Factors (% explained variability) | Cumulative explained variability (%) |
|---|---|---|
| All sites (Red Forest and Buriakivka) (N = 55) | Site type (15.43); spatial distance (8.66); pH (3.52); burn (2.97); LOI (2.23); other veg DM (2.02); $NO_3$ (1.99); soil moisture (2.10); **BDR (1.87)**; biological activity (1.42) | 42.22 |
| Red Forest (N = 49) | Spatial distance (17.19); burn (4.19); pH (3.86); site type (3.45); LOI (2.56); $NO_3$ (2.26); soil moisture (2.40); other veg. DM (2.28) **BDR (2.16)** | 40.34 |
| Unplanted (N = 19) | pH (21.88); spatial distance (14.35.); burn (11.06); soil moisture (5.06) | 52.35 |
| Planted (N = 30) | Spatial distance (11.27); soil moisture (6.85) | 18.10 |

other vegetation dry mass and $NO_3$ were included in the All Sites and Red Forest models, while biological activity was only included in the All Sites model. Fitting BDR before burn changed very little the amount of variation explained by BDR (0.38 %), in contrast to the change caused by fitting BDR before spatial distance (17.59 %), $NO_3$ (5.70 %) and site type (4.60 %), followed by LOI (2.34 %), other vegetation dry mass (2.03 %), pH (1.78 %) and soil moisture (0.98) (Table 4).

**Table 4**

Change in variation explained by BDR when fitted before and after each significant DistLM variable included in Red Forest model, Aitchinson distance. Each tested variable was fitted before and then after BDR once all other variables had been fitted in the model. Values shown in BDR explained variation column is the BDR explained variation when fitted before tested variable. LOI = loss on ignition; O. veg. DM = other vegetation dry mass.

| Variable tested | BDR explained variation | % change |
|---|---|---|
| Burn | 2.15 | 0.38 |
| Spatial distance | 2.54 | 17.59 |
| pH | 2.20 | 1.78 |
| LOI | 2.21 | 2.34 |
| NO$_3$ | 2.04 | 5.70 |
| Soil moisture | 2.14 | 0.98 |
| O. veg. DM | 2.12 | 2.03 |
| Site type | 2.06 | 4.60 |

*3.7. Co-occurrence network analysis*

The Red Forest soil microbial co-occurrence network had 6 modules, two of which, modules 3 and 6, showed strong positive correlations with radiation (correlation with GDR r > 0.5, p < 0.0001) (Fig. 4). These modules had statistically significant negative correlation with soil moisture and biological activity (module 6), and with soil pH and biological activity (module 3). While modules 3 and 6 were positively correlated with all dose rates, module 3 had stronger correlations with ADR and GDR, while module 6 had stronger correlation with GDR than ADR. Correlations with TDR and BDR were positive however the p-values were considerably weaker or not significant. One module (module 1) showed statistically significant negative correlation with radiation, and this module was strongly correlated with soil pH, moisture, nitrate, total vegetation dry mass and biological activity data.

At phylum level, it was noticeable that 10.75 % of ASVs in module 1 were classified to Firmicutes, while only 0.4 and 0 % of ASVs were classified to this Phylum in the modules 3 and 6, respectively (Table S3). Module 6 had considerably lower number of ASVs classified to Acidobacteria (6.37 %) and Verrucomicrobia (0.49 %) and double the percentage classified to Actinobacteria (24.51 %) and Chloroflexi (10.78 %) compared to module 1 (14.02, 4.21, 14.49 and 6.54 % for Acidobacteria, Verrucomicrobia, Actinobacteria and Chloroflexi, respectively) and module 3 (12.76, 5.76, 12.35 and 5.35 % for Acidobacteria, Verrucomicrobia, Actinobacteria and Chloroflexi, respectively). ASVs classified

to the WPS-2 phylum were more important in modules 3 and 6 compared to module 1. ASVs classified to the WPS-2 phylum were 5.35 and 7.35 % of ASVs in modules 3 and 6, respectively, but only 1.87 % of module 1.

There were 41 ASVs that had significant Pearson correlations (q values <0.05) to one or more dose rates (GDR, ADR, BDR or TDR) and which had no significant q value to non-radiation soil variables (Supplementary Fig. S3). Of these, 29 correlated to GDR, 27 to ADR, 24 to BDR and 15 to TDR, with many ASVs correlating to multiple dose rates. Of these ASVs, 37 were negative and 4 positive correlations. The 4 ASVs with positive correlations to dose rates were classified to P_WPS-2 (correlated to ADR and TDR), F_LWQ8 (Saccharimonadale, Patescibacteria, correlated to ADR and TDR), *Actinomadura* (Actinobacteria, correlated to GDR), and F_Micropepsaceae (Alphaproteobacteria, correlated to GDR and ADR). The ASVs with negative correlations to dose rates were classified to a diverse set of microbial groups, with 10 each being classified to the Actinobacteriota and Planctomycetota, 9 to the Proteobacteria, and 3 to the Acidobacteria and Armatimonadota each and 1 each to the Chloroflexi and WPS-2. Of the ASVs that were classified to a genus, these included several members of the Actinobacteria class (e.g. *Catenulispora*, *Kineosporia*, *Jatrophihabitans*, *Pseudonocardia*, *Acidothermus*), as well as *Aquisphaera*, *Chthonomonas*, *Edaphobacter*, *Gemmata*, *Novosphingobium*, *Pandoraea* and *Roseiarcus*. Interestingly, only 1 Chloroflexi, 1 WPS-2 and no Verrucomicrobia ASVs were included among these 41 taxa, despite their importance in the Red Forest microbiome (Supplementary Fig. S1). Of the ASVs, 32 belonged to module 4, 4 to module 6, 2 each to modules 5 and 1, and 1 to module 2. Ten of the 41 ASVs (24 %) correlated with all dose rates, while 12 (29 %) correlated only with GDR, 3 (7 %) and 2 (5 %) correlated to ADR and BDR only and no ASV correlated to TDR only (Supplementary Fig. S3).

**4. Discussion**

In this study, we investigated the relationship between ambient dose rates and estimated total absorbed dose rates to grass, bacteria and trees as well as land use history, wildfire and soil conditions on the soil microbiome at the CEZ. The links between radiation and soil microbiome appear relatively weak once co-variation with soil properties and distance are considered. The presence of stress-tolerating microbial groups may partly explain the weak effects of radiation on the soil microbial community structure. These findings represent a first step
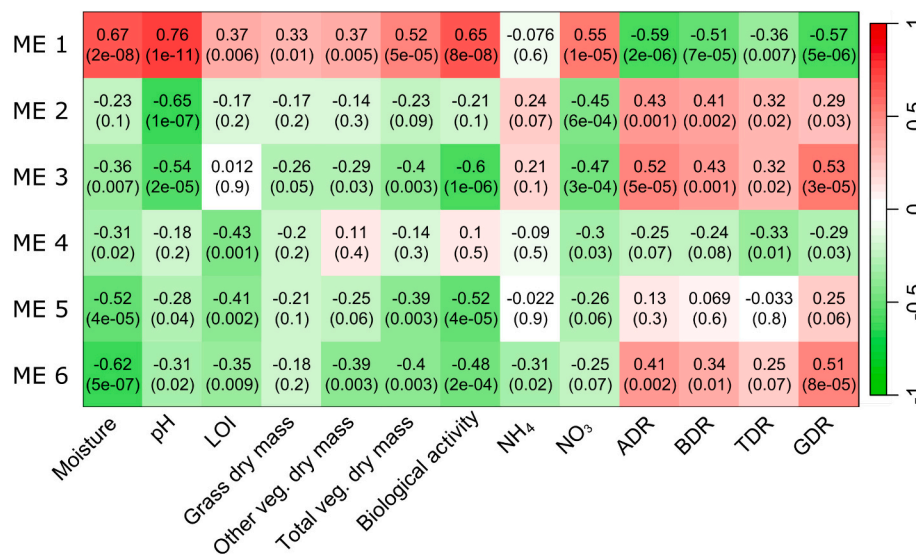


**Fig. 4.** Heatmap showing the strength of correlations between microbial modules, soil variables and radiation dose rates. ME = module eigengene for each module. LOI = loss on ignition; ADR = ambient dose rate; BDR, TDR and GDR = absorbed dose rates to bacteria, trees and grassy vegetation, respectively. The correlation (r) is shown for each correlation and the p values are in brackets.

towards a better understanding of the effects of chronic high radiation on the soil microbial communities at the CEZ.

### 4.1. Effects of soil moisture and wildfire on microbial ß-diversity

Multivariate dispersion analysis showed that heterogeneity in microbial ß-diversity in the Red Forest region was higher in the Unplanted sites. This is likely related to differences in soil moisture and pH, with the most dissimilar Unplanted samples corresponding to those forming outlying clusters in the nMDS plot with higher moisture and soil pH compared to the other Red Forest samples and Buriakivka. In addition, dispersion of microbial communities was greater for Burn than No Burn. A recent study found that wildfire led to reduced dispersion in the top 5 cm of soil but increased dispersion in the bottom 5–10 cm soil (Nelson et al., 2022). The increased dispersion in the bottom 5–10 cm soil was attributed to greater stochastic shifts in microbial communities associated with uneven changes in soil chemistry and nutrient availability at depth (Nelson et al., 2022). In the present study, the soils were collected from the surface down to 10 cm, and the observation of increased dispersion of Burn soil's microbial community may similarly be associated with increased importance of stochasticity in the microbial community assembly processes at depth. Furthermore, it is possible that the higher dispersion of Burn sites was related to variation in soil moisture in the Unplanted samples. All the Unplanted samples with high moisture and high soil pH forming distinct outlying clusters in the nMDS plot were also Burn samples. Higher soil moisture may have changed the effect of fire in soil properties (Agbeshie et al., 2022), affecting the speed with which the soil microbial community recovered post fire compared to the low moisture samples, where the drier soils may have slowed microbial recovery (Köster et al., 2021). This is in agreement with a previous study that showed variations in dispersion over time following a forest fire (Prendergast-Miller et al., 2017). Hence, in the higher moisture soils, the faster microbial recovery post-fire would have changed soil microbial community structure to a greater extent relative to the No Burn soils.

### 4.2. Stress-tolerating microbial groups in the CEZ soil

Ordination analysis showed that most of the Planted and Unplanted samples with higher radiation contamination tended to cluster together, and these samples also tended to be lower in soil moisture and with more acidic soil pH and lower vegetation dry mass. The microbial groups that correlated with the high radiation Red Forest samples (including both Planted and Unplanted samples) in the nMDS plot included groups that have previously been associated with stress-tolerator traits, or adaptations to harsher ecological conditions. For example, the Ktedonobacteria class (Chloroflexi) have been associated with metal contaminated soils (Yamada and Sekiguchi, 2009), the Isosphaeraceae (Planctomycetes) have been found to increase in abundance following application of polycyclic aromatic hydrocarbons (Zhao et al., 2016), the Acidothermaceae family contains thermophilic members (Berry et al., 2014), and the WPS-2 phyla have been associated with acidic, dry, bare, metal-contaminated soils (Sheremet et al., 2020), organic-poor soils such as Antarctic (Ji et al., 2017), Arctic surface aggregates (Stibal et al., 2015) and dry, volcanic soils (Costello et al., 2009). Environmental members of the *Mycobacterium* genus are known to be capable of breaking down toxic organic pollutants (Storey et al., 2018), they have a unique outer membrane that renders their cells hydrophobic and is thought to protect their cells against harmful compounds (Boot et al., 2017), and are known to frequently inhabit harsh environments (Kołodziej et al., 2021).

### 4.3. Soil total absorbed dose rates to bacteria and known microbial radiation resistance

Microbial radiation resistance has been studied extensively, however, in most cases these studies were carried out in laboratory conditions and used dose rates orders of magnitude higher (in the kGy range)

than what is observed in the most contaminated samples in the CEZ's Red Forest (BDR up to 4600 μGy h$^{-1}$). Reported gamma radiation doses for 1 log cycle reduction in bacterial survival vary from <1 kGy to >5 kGy (Singh, 2018). Few studies reported the effects of low radiation doses on microbial metabolism, however, a recent study investigated doses of 10 mGy d$^{-1}$ delivered to *E. coli* over 1 or 15 days (Wintenberg et al., 2023). That study found widespread transcriptional changes in the *E. coli* cells as a result of both the shorter and longer term 10 mGy d$^{-1}$ exposures, with differential expression of genes related to biosynthesis of nuclear envelope components, amino acids, siderophores, ABC transport and type II secretion systems, as well as initiation of stress responses, including temperature and oxidative stress response. Therefore, the BDR estimates for the Red Forest soil (up to 110 mGy d$^{-1}$) were potentially sufficient to impact the metabolism of the soil microbiome. However, the impact of radiation in organisms observed in laboratory studies are often not observed under field conditions (Beresford et al., 2020b), and the native soil microbiome may have greater resistance to radiation than *E. coli*, given the exposure to other sources of oxidative stress, particularly desiccation, which share resistance mechanisms with ionising radiation (Daly, 2023; Singh, 2018). Indeed, the harsh environmental conditions of many samples in the Red Forest, in particular low soil moisture, likely selected for microorganisms with stress resistance traits, and the microbial population there may be considerably more resistant to ionising radiation compared to *E. coli* strains growing under laboratory conditions. This contrasts with the findings of a study comparing the radiosensitivity of wildlife in Chornobyl with data from controlled radiation exposure experiments (Garnier-Laplace et al., 2013). According to the latter study, Chornobyl wildlife appeared to be more radiosensitive than those in controlled studies. However, the study concluded that further research is needed to determine how confounding factors affect wildlife radiosensitivity in the field. The data used by Garnier-Laplace et al. (2013) was from multicellular organisms (terrestrial animals and plants) only, and how their findings can be applied to microorganisms directly exposed to soil conditions is unclear at present.

### 4.4. Links between radiation contamination and soil microbial community structure

Overall, ADR was more important in explaining variation in microbial communities than estimated total absorbed dose rates to grass, bacteria and trees, as evidenced by ADR being included more often in the Red Forest and Unplanted sites' DistLM models. Dose rates were not retained in DistLM models for the Planted sites, which is surprising given that dose rates there were considerably higher than those of the Unplanted sites. It is noteworthy that, in contrast to models for Unplanted sites, Red Forest and All Sites, the total explained variation was considerably lower for Planted sites and only spatial distance and soil moisture were included in the final models. The Planted sites may have experienced greater environmental stress as their lower levels of soil moisture, total vegetation dry mass, and nitrate levels are associated with higher environmental stress (Hernandez et al., 2021). Environmental stress increases the proportion of dormant or senescent cells within microbial communities (Blagodatskaya and Kuzyakov, 2013). Due to the higher proportion of dormant or senescent microbial cells, a greater proportion of the extracted DNA could come from inactive cells, which may be less representative of environmental conditions at the time of sampling, and hence reduce our ability to detect radiation-soil microbial community relationships. Furthermore, microbial adaptation to environmental stresses in these sites may have favoured microbial taxa with high stress resistance traits and consequently with greater resistance to ionising radiation (Shuryak, 2019). Nevertheless, it is apparent that any impact of radiation on the soil microbiome in the Planted sites is relatively weak despite the higher radiation levels observed there.

ADR was the only dose rate included in the Unplanted sites final

DistLM models. However, ADR is determined using a beta-shielded dosimeter that is placed above the soil, without considering the radionuclide transfer rates and the internal absorbed radiation organisms are exposed to or, in the case of microorganisms, the external dose contribution from the actinides that are prevalent in CEZ soils. ADR only accounts for external exposure and therefore is less representative of the amount of radiation specific organisms are exposed to in the CEZ (Burraco et al., 2021). In contrast, GDR, TDR and BDR were determined based on measured soil radionuclide activity concentrations, radionuclide transfer rates for grasses, trees (calculated from the CEZ data), and dosimetry parameter values that reflect the external dose contribution of actinides to bacteria (Barnett et al., 2021). There remains a possibility that radiation is affecting the soil microbiome as BDR, TDR and to a lesser extent GDR were included in some final DistLM models explaining similar levels of variation as NO₃, LOI and other vegetation dry mass. However, this apparent relationship between radiation and soil microbial community structure in the present study must be viewed with caution given the general trend in the Red Forest of higher radionuclide deposition in areas with drier and more acidic soils.

Changes in explained variation by BDR when fitted before and after other significant DistLM model variables was carried out to assess the extent of overlap between the variation in the soil microbiome that is explained by BDR, burn and other soil variables (Anderson et al., 2008). This analysis showed that fitting burn before and after BDR made very little difference to the BDR explained variability. Interestingly, burn was the variable that least overlapped with BDR's explained variability. The lack of co-variation in explained variability between BDR and burn argues against a relationship between the effects of burn and BDR on the soil microbiome.

### 4.5. Microbial co-occurrence network analysis

Co-occurrence analysis revealed that 3 out of 6 modules correlated positively or negatively to radiation with a p value <0.0001. Interestingly, modules positively correlated to dose rates were negatively correlated to soil moisture and/or soil pH, and vice versa. This reflects the general trend in the Red Forest of higher radiation contamination being found in soils that can be considered harsher (drier and with more acidic pH). Hence, spatial co-correlation between radiation, soil moisture, soil pH, vegetation and biological activity likely contributed to the module-soil variable relationships identified. The correlation between individual microbial ASVs and dose rates revealed a selection of 41 taxa which had significant correlations to dose rates only, most of which (37 of 41) were negative correlations. As with the DistLM, the small number of taxa uniquely correlated to radiation relative to the total number of taxa (26,708) highlight that any effects of radiation on the CEZ soil microbiome are likely to be small.

Some previous studies have suggested that radiation is having an impact in soil microbial processes, such as decomposition, in the CEZ (Bonzom et al., 2016; Mousseau et al., 2014). Of the radiation-correlated ASVs that were classified to a genus, these included several members of the class Actinobacteria, which are known for their saprotrophic traits (Goodfellow et al., 2012), and other taxa that are similarly associated with decomposition of organic matter or plant cell wall breakdown such as *Gemmata* (Ivanova et al., 2018), family Isosphaeraceae (Ivanova et al., 2017), WD2101 soil group (Dedysh et al., 2021), *Chthonomonas* (Lee et al., 2014) and *Edaphobacter* (Eichorst et al., 2018). Taxa that have been implicated in the breakdown of aromatic and xenobiotic compounds, e.g. *Novosphingobium* (Wang et al., 2018) and *Pandoraea* (Peeters et al., 2019) were also among those correlating negatively with dose rates. This indicates a possible link between radiation levels and organic carbon cycling in the Red Forest. However, as previously noted, it is clear that other variables, notably site type, distance and soil pH, rather that radiation per se, are driving the microbial community structure in the sites studied.

## 5. Conclusions

The CEZ region is a unique location to carry out ecosystem-level studies of the long-term impact of chronic radiation on biodiversity and ecosystem processes. In the CEZ, the soil microbial communities are exposed to environmental stress associated with variations in soil conditions, such as acidic pH, low soil moisture or lack of nutrients. This enables an assessment of the relative importance of radiation relative to other environmental stresses under in-situ conditions. The variables that affected the soil microbiome the most were site type (Buriakivka, Planted or Unplanted), spatial distance, soil pH, burn and soil moisture. Wildfire appeared to increase variability of the soil microbial communities, which is possibly linked to variations in soil moisture affecting the post-fire ecological recovery. There was no relationship between the effects of wildfire and radiation on the soil microbiome. DistLM and co-occurrence analysis both indicated that the effects of radiation on the soil microbiome in the Red Forest region are minimal, despite BDR reaching levels that can significantly affect microbial metabolism in laboratory experiments. The lack of stronger relationships between total absorbed dose rates to grass, trees and bacteria suggest that the Red Forest soil microbiome is mostly resistant or has adapted to current direct and indirect effects of radiation. This may be a result of microbial adaptation to the generally high environmental stress conditions of the Red Forest soil, in particular the drier and more acidic pH soils that tend to be associated with the higher radionuclide deposition areas. Future studies across multiple years and seasons with additional sampling sites across the CEZ are needed to fully address the confounding effects of spatial and temporal variation in our understanding of soil microbiome responses to chronic radiation at the CEZ. Further, experimental manipulation of plant cover and soil are needed to establish whether radiation impacts on above-ground plant communities have indirect effects on the soil microbial communities and microbial ecosystem processes.

## CRediT authorship contribution statement

**Alexandre Barretto de Menezes:** Writing – review & editing, Writing – original draft, Visualization, Methodology, Investigation, Funding acquisition, Formal analysis, Data curation, Conceptualization. **Sergii Gashchak:** Writing – review & editing, Project administration, Methodology, Investigation. **Michael D. Wood:** Writing – review & editing, Project administration, Methodology, Investigation, Funding acquisition, Conceptualization. **Nicholas A. Beresford:** Writing – review & editing, Project administration, Methodology, Investigation, Funding acquisition, Conceptualization.

## Declaration of competing interest

The authors declare that they have no known competing financial interests or personal relationships that could have appeared to influence

the work reported in this paper.

## Appendix A. Supplementary data

Supplementary data to this article can be found online at https://doi.org/10.1016/j.scitotenv.2024.175381.

## References

Agbeshie, A.A., Abugre, S., Atta-Darkwa, T., Awuah, R., 2022. A review of the effects of forest fire on soil properties. J. For. Res. 33, 1419–1441. https://doi.org/10.1007/s11676-022-01475-4.

Alexakhin, R.M., Sanzharova, N.I., Fesenko, S.V., Spiridonov, S.I., Panov, A.V., 2007. Chernobyl radionuclide distribution, migration, and environmental and agricultural impacts. Health Phys. 93, 418–426. https://doi.org/10.1097/01.HP.0000285093.63814.b7.

Allen, S.E., 1974. Chemical Analysis of Ecological Materials. Blackwell Scientific Publications, Oxford and London.

Anderson, M.J., Gorley, R.N., Clarke, K.R., 2008. PERMANOVA+ for PRIMER: Guide to Software and Statistical Methods. PRIMER-E Ltd, Plymouth, UK.

Antwis, R.E., Beresford, N.A., Jackson, J.A., Fawkes, R., Barnett, C.L., Potter, E., Walker, L., Gaschak, S., Wood, M.D., 2021. Impacts of radiation exposure on the bacterial and fungal microbiome of small mammals in the Chernobyl Exclusion Zone. J. Anim. Ecol. 1–16. https://doi.org/10.1111/1365-2656.13507.

Barnett, C.L., Gashchak, S., Maksimenko, A., Chaplow, J.S., Wood, M.D., Beresford, N.A., 2021. Soil and Vegetation Radionuclide Activity Concentrations and Calculated Dose Rates From the Red Forest, Chernobyl, Ukraine, 2016-2017. https://doi.org/10.5285/60782622-7bfa-4615-a9e3-0a802a9f4674.

Beresford, N.A., Barnett, C.L., Gashchak, S., Maksimenko, A., Guliaichenko, E., Wood, M.D., Izquierdo, M., 2020a. Radionuclide transfer to wildlife at a 'Reference site' in the Chernobyl Exclusion Zone and resultant radiation exposures. J. Environ. Radioact. 211, 105661 https://doi.org/10.1016/j.jenvrad.2018.02.007.

Beresford, N.A., Horemans, N., Copplestone, D., Raines, K.E., Orizaola, G., Wood, M.D., Laanen, P., Whitehead, H.C., Burrows, J.E., Tinsley, M.C., Smith, J.T., Bonzom, J.-M., Gagnaire, B., Adam-Guillermin, C., Gashchak, S., Jha, A.N., de Menezes, A., Willey, N., Spurgeon, D., 2020b. Towards solving a scientific controversy – the effects of ionising radiation on the environment. J. Environ. Radioact. 211, 106033 https://doi.org/10.1016/j.jenvrad.2019.106033.

Beresford, N.A., Barnett, C.L., Gashchak, S., Kashparov, V., Kirieiev, S.I., Levchuk, S., Morozova, V., Smith, J.T., Wood, M.D., 2021. Wildfires in the Chornobyl Exclusion Zone – risks and consequences. Integr. Environ. Assess. Manag. 00, 1–10. https://doi.org/10.1002/ieam.4424.

Beresford, N.A., Wood, M.D., Gashchak, S., Barnett, C.L., 2022. Current ionising radiation doses in the Chernobyl Exclusion Zone do not directly impact on soil biological activity. PLoS One 17, e0263600. https://doi.org/10.1371/journal.pone.0263600.

Berry, A.M., Barabote, R.D., Normand, P., 2014. The family Acidothermaceae, in: The Prokaryotes: Actinobacteria. Rosenberg, E., DeLong, E.F., Lory, S., Stackebrandt, E., Thompson, F. (eds). Berlin, Heidelberg, Germany: Springer Berlin Heidelberg, pp. 13–19. doi:https://doi.org/10.1007/978-3-642-30138-4_199.

Blagodatskaya, E., Kuzyakov, Y., 2013. Active microorganisms in soil: critical review of estimation criteria and approaches. Soil Biol. Biochem. 67, 192–211. https://doi.org/10.1016/j.soilbio.2013.08.024.

Bonzom, J.M., Hattenschwiler, S., Lecomte-Pradines, C., Chauvet, E., Gaschak, S., Beaugelin-Seiller, K., Della-Vedova, C., Dubourg, N., Maksimenko, A., Garnier-Laplace, J., Adam-Guillermin, C., 2016. Effects of radionuclide contamination on leaf litter decomposition in the Chernobyl exclusion zone. Sci. Total Environ. 562, 596–603. https://doi.org/10.1016/j.scitotenv.2016.04.006.

Boot, M., van Winden, V.J.C., Sparrius, M., van de Weerd, R., Speer, A., Ummels, R., Rustad, T., Sherman, D.R., Bitter, W., 2017. Cell envelope stress in mycobacteria is regulated by the novel signal transduction ATPase IniR in response to trehalose. PLoS Genet. 13, e1007131 https://doi.org/10.1371/journal.pgen.1007131.

Boubriak, I., Akimkina, T., Polischuk, V., Dmitriev, A., McCready, S., Grodzinsky, D., 2016. Long term effects of Chernobyl contamination on DNA repair function and

plant resistance to different biotic and abiotic stress factors. Cytol. Genet. 50, 381–399. https://doi.org/10.3103/S0095452716060049.

Brown, J.E., Alfonso, B., Avila, R., Beresford, N.A., Copplestone, D., Pröhl, G., Ulanovsky, A., 2008. The ERICA Tool. J. Environ. Radioact. 99, 1371–1383. https://doi.org/10.1016/j.jenvrad.2008.01.008.

Brown, J.E., Alfonso, B., Avila, R., Beresford, N.A., Copplestone, D., Hosseini, A., 2016. A new version of the ERICA tool to facilitate impact assessments of radioactivity on wild plants and animals. J. Environ. Radioact. 153, 141–148. https://doi.org/10.1016/j.jenvrad.2015.12.011.

Burraco, P., Car, C., Bonzom, J.M., Orizaola, G., 2021. Assessment of exposure to ionizing radiation in Chernobyl tree frogs (*Hyla orientalis*). Sci. Rep. 11, 1–10. https://doi.org/10.1038/s41598-021-00125-9.

Callahan, B.J., Sankaran, K., Fukuyama, J.A., McMurdie, P.J., Holmes, S.P., 2016. Bioconductor workflow for microbiome data analysis: from raw reads to community analyses. F1000Research 5, 1492. https://doi.org/10.12688/f1000research.8986.1.

Caporaso, J.G., Lauber, C.L., Walters, W.A., Berg-Lyons, D., Lozupone, C.A., Turnbaugh, P.J., Fierer, N., Knight, R., 2011. Global patterns of 16S rRNA diversity at a depth of millions of sequences per sample. Proc. Natl. Acad. Sci. USA 108 (Suppl), 4516–4522. https://doi.org/10.1073/pnas.1000080107.

Cobo-Díaz, J.F., Fernández-González, A.J., Villadas, P.J., Robles, A.B., Toro, N., Fernández-López, M., 2015. Metagenomic assessment of the potential microbial nitrogen pathways in the rizosphere of a Mediterranean forest after a wildfire. Microb. Ecol. 69, 895–904. https://doi.org/10.1007/s00248-015-0586-7.

Copplestone, D., Bielby, S., Jones, S.R., Patton, D., Daniel, P., Gize, I., 2001. Impact assessment of ionising radiation on wildlife. Environ. Agency RD Publ. 128, 1–222.

Costello, E.K., Halloy, S.R.P., Reed, S.C., Sowell, P., Schmidt, S.K., 2009. Fumarole-supported islands of biodiversity within a hyperarid, high-elevation landscape on Socompa Volcano, Puna de Atacama, Andes. Appl. Environ. Microbiol. 75, 735–747. https://doi.org/10.1128/AEM.01469-08.

Daly, M.J., 2023. The scientific revolution that unraveled the astonishing DNA repair capacity of the *Deinococcaceae*: 40 years on. Can. J. Microbiol. 69, 369–386. https://doi.org/10.1139/cjm-2023-0059.

Dedysh, S.N., Beletsky, A.V., Ivanova, A.A., Kulichevskaya, I.S., Suzina, N.E., Philippov, D.A., Rakitin, A.L., Mardanov, A.V., Ravin, N.V., 2021. Wide distribution of *Phycisphaera*-like planctomycetes from WD2101 soil group in peatlands and genome analysis of the first cultivated representative. Environ. Microbiol. 23, 1510–1526. https://doi.org/10.1111/1462-2920.15360.

Dixon, P., 2003. VEGAN, a package of R functions for community ecology. J. Veg. Sci. 14, 927–930. https://doi.org/10.1111/j.1654-1103.2003.tb02228.x.

Dooley, S.R., Treseder, K.K., 2012. The effect of fire on microbial biomass: a meta-analysis of field studies. Biogeochemistry 109, 49–61. https://doi.org/10.1007/s10533-011-9633-8.

Eichorst, S.A., Trojan, D., Roux, S., Herbold, C., Rattei, T., Woebken, D., 2018. Genomic insights into the *Acidobacteria* reveal strategies for their success in terrestrial environments. Environ. Microbiol. 20, 1041–1063. https://doi.org/10.1111/1462-2920.14043.

Flannigan, M.D., Krawchuk, M.A., de Groot, W.J., Wotton, B.M., Gowman, L.M., 2009. Implications of changing climate for global wildland fire. Int. J. Wildland Fire 18, 483. https://doi.org/10.1071/WF08187.

Garnier-Laplace, J., Geras'kin, S., Della-Vedova, C., Beaugelin-Seiller, K., Hinton, T.G., Real, A., Oudalova, A., 2013. Are radiosensitivity data derived from natural field conditions consistent with data from controlled exposures? A case study of Chernobyl wildlife chronically exposed to low dose rates. J. Environ. Radioact. 121, 12–21. https://doi.org/10.1016/j.jenvrad.2012.01.013.

Geras'kin, S., Evseeva, T., Oudalova, A., 2013. Effects of long-term chronic exposure to radionuclides in plant populations. J. Environ. Radioact. 121, 22–32. https://doi.org/10.1016/j.jenvrad.2012.03.007.

Goodfellow, M., Kämpfer, P., Busse, H.-J., Trujillo, M.E., Suzuki, K., Ludwig, W., Whitman, W.B. (Eds.), 2012. Bergey's Manual of Systematic Bacteriology. Volume 5, the Actinobacteria, Second edition. New York, Springer.

Hernandez, D.J., David, A.S., Menges, E.S., Searcy, C.A., Afkhami, M.E., 2021. Environmental stress destabilizes microbial networks. ISME J. 15, 1722–1734. https://doi.org/10.1038/s41396-020-00882-x.

Holiaka, D., Fesenko, S., Kashparov, V., Protsak, V., Levchuk, S., Holiaka, M., 2020a. Effects of radiation on radial growth of Scots pine in areas highly affected by the Chernobyl accident. J. Environ. Radioact. 222, 106320 https://doi.org/10.1016/j.jenvrad.2020.106320.

Holiaka, D.M., Levchuk, S.E., Yoschenko, V.I., Kashparov, V.A., Yoschenko, L.V., Holiaka, M.A., Pavliuchenko, V.V., Diachuk, P.P., Zadorozhniuk, R.M., Morozova, V.S., 2020b. $^{90}$Sr and $^{137}$Cs inventories in the depots and biogenic fluxes of the typical forest stands in the Chernobyl exclusion zone. Nucl. Phys. At. Energy 21, 256–264. https://doi.org/10.15407/jnpae2020.03.256.

Hoyos-Hernandez, C., Courbert, C., Simonucci, C., David, S., Vogel, T.M., Larose, C., 2019. Community structure and functional genes in radionuclide contaminated soils in Chernobyl and Fukushima. FEMS Microbiol. Lett. 366, 1–10. https://doi.org/10.1093/femsle/fnz180.

International Atomic Energy Agency, 2006. Environmental consequences of the Chernobyl accident and their remediation: twenty years of experience. In: Radiological Assessment Reports Series.

Ivanova, A.A., Naumoff, D.G., Miroshnikov, K.K., Liesack, W., Dedysh, S.N., 2017. Comparative genomics of four Isosphaeraceae Planctomycetes: a common pool of plasmids and glycoside hydrolase genes shared by *Paludisphaera borealis* PX4T, *Isosphaera pallida* IS1BT, *Singulisphaera acidiphila* DSM 18658T, and strain SH-PL62. Front. Microbiol. 8, 412. https://doi.org/10.3389/fmicb.2017.00412.

Ivanova, A.A., Wegner, C.-E., Kim, Y., Liesack, W., Dedysh, S.N., 2018. Metatranscriptomics reveals the hydrolytic potential of peat-inhabiting

Planctomycetes. Antonie Van Leeuwenhoek 111, 801–809. https://doi.org/10.1007/s10482-017-0973-9.

Ji, M., Greening, C., Vanwonterghem, I., Carere, C.R., Bay, S.K., Steen, J.A., Montgomery, K., Lines, T., Beardall, J., van Dorst, J., Snape, I., Stott, M.B., Hugenholtz, P., Ferrari, B.C., 2017. Atmospheric trace gases support primary production in Antarctic desert surface soil. Nature 552, 400–403. https://doi.org/10.1038/nature25014.

Jost, L., 2006. Entropy and diversity. Oikos 113, 363–375. https://doi.org/10.1111/j.2006.0030-1299.14714.x.

Jung, K.-W., Lim, S., Bahn, Y.-S., 2017. Microbial radiation-resistance mechanisms. J. Microbiol. 55, 499–507. https://doi.org/10.1007/s12275-017-7242-5.

Kołodziej, M., Łebkowski, T., Płociński, P., Hołówka, J., Paściak, M., Wojtaś, B., Bury, K., Konieczny, I., Dziadek, J., Zakrzewska-Czerwińska, J., 2021. Lsr2 and its novel paralogue mediate the adjustment of *Mycobacterium smegmatis* to unfavorable environmental conditions. mSphere 6. https://doi.org/10.1128/msphere.00290-21.

Köster, K., Aaltonen, H., Berninger, F., Heinonsalo, J., Köster, E., Ribeiro-Kumara, C., Sun, H., Tedersoo, L., Zhou, X., Pumpanen, J., 2021. Impacts of wildfire on soil microbiome in boreal environments. Curr. Opin. Environ. Sci. Health 22, 100258. https://doi.org/10.1016/j.coesh.2021.100258.

Kruskal, W.H., Wallis, W.A., 1952. Use of ranks in one-criterion variance analysis. J. Am. Stat. Assoc. 47, 583–621. https://doi.org/10.2307/2280779.

Kuchma, O., Finkeldey, R., 2011. Evidence for selection in response to radiation exposure: *Pinus sylvestris* in the Chernobyl exclusion zone. Environ. Pollut. 159, 1606–1612. https://doi.org/10.1016/j.envpol.2011.02.049.

Langfelder, P., Horvath, S., 2008. WGCNA: an R package for weighted correlation network analysis. BMC Bioinformatics 9, 559. https://doi.org/10.1186/1471-2105-9-559.

Lavrinienko, A., Mappes, T., Tukalenko, E., Mousseau, T.A., Møller, A.P., Knight, R., Morton, J.T., Thompson, L.R., Watts, P.C., 2018. Environmental radiation alters the gut microbiome of the bank vole Myodes glareolus. ISME J. 12, 2801–2806. https://doi.org/10.1038/s41396-018-0214-x.

Lavrinienko, A., Tukalenko, E., Kesäniemi, J., Kivisaari, K., Masiuk, S., Boratyński, Z., Mousseau, T.A., Milinevsky, G., Mappes, T., Watts, P.C., 2020. Applying the Anna Karenina principle for wild animal gut microbiota: temporal stability of the bank vole gut microbiota in a disturbed environment. J. Anim. Ecol. 89, 2617–2630. https://doi.org/10.1111/1365-2656.13342.

Lavrinienko, A., Hämäläinen, A., Hindström, R., Tukalenko, E., Boratyński, Z., Kivisaari, K., Mousseau, T.A., Watts, P.C., Mappes, T., 2021. Comparable response of wild rodent gut microbiome to anthropogenic habitat contamination. Mol. Ecol. 30, 3485–3499. https://doi.org/10.1111/mec.15945.

Lecomte-Pradines, C., Adam-Guillermin, C., Gashchak, S., Bradshaw, C., Copplestone, D., Beresford, N.A., 2020. More than thirty years after the Chernobyl accident: what do we know about the effects of radiation on the environment? J. Environ. Radioact. 211, 106108 https://doi.org/10.1016/j.jenvrad.2019.106108.

Lee, K.C.-Y., Morgan, X.C., Dunfield, P.F., Tamas, I., McDonald, I.R., Stott, M.B., 2014. Genomic analysis of *Chthonomonas calidirosea*, the first sequenced isolate of the phylum Armatimonadetes. ISME J. 8, 1522–1533. https://doi.org/10.1038/ismej.2013.251.

Lin, H., Peddada, S.D., 2020. Analysis of compositions of microbiomes with bias correction. Nat. Commun. 1–11. https://doi.org/10.1038/s41467-020-17041-7.

McNamara, N.P., Griffiths, R.I., Tabouret, A., Beresford, N.A., Bailey, M.J., Whiteley, A. S., 2007. The sensitivity of soil microbial community to acute gamma-irradiation. Appl. Soil Ecol. 37, 1–9. https://doi.org/10.1016/j.apsoil.2007.03.011.

de Menezes, A.B., Prendergast-Miller, M.T., Macdonald, L.M., Toscas, P., Baker, G., Farrell, M., Wark, T., Richardson, A.E., Thrall, P.H., 2018. Earthworm-induced shifts in microbial diversity in soils with rare versus established invasive earthworm populations. FEMS Microbiol. Ecol. 94, 1–14. https://doi.org/10.1093/femsec/fiy051.

Mothersill, C.E., Oughton, D.H., Schofield, P.N., Abend, M., Adam-Guillermin, C., Ariyoshi, K., Beresford, N.A., Bonisoli-Alquati, A., Cohen, J., Dubrova, Y., Geras'kin, S.A., Hevrøy, T.H., Higley, K.A., Horemans, N., Jha, A.N., Kapustka, L.A., Kiang, J.G., Madas, B.G., Powathil, G., Sarapultseva, E.I., Seymour, C.B., Vo, N.T.K., Wood, M.D., 2022. From tangled banks to toxic bunnies; a reflection on the issues involved in developing an ecosystem approach for environmental radiation protection. Int. J. Radiat. Biol. 98, 1185–1200. https://doi.org/10.1080/09553002.2020.1793022.

Mousseau, T.A., Milinevsky, G., Kenney-Hunt, J., Møller, A.P., 2014. Highly reduced mass loss rates and increased litter layer in radioactively contaminated areas. Oecologia 175, 429–437. https://doi.org/10.1007/s00442-014-2908-8.

Nelson, A.R., Narrowe, A.B., Rhoades, C.C., Fegel, T.S., Daly, R.A., Roth, H.K., Chu, R.K., Amundson, K.K., Young, R.B., Steindorff, A.S., Mondo, S.J., Grigoriev, I.V., Salamov, A., Borch, T., Wilkins, M.J., 2022. Wildfire-dependent changes in soil microbiome diversity and function. Nat. Microbiol. 7, 1419–1430. https://doi.org/10.1038/s41564-022-01203-y.

Newbold, L.K., Robinson, A., Rasnaca, I., Lahive, E., Soon, G.H., Lapied, E., Oughton, D., Gashchak, S., Beresford, N.A., Spurgeon, D.J., 2019. Genetic, epigenetic and microbiome characterisation of an earthworm species (*Octolasion lacteum*) along a radiation exposure gradient at Chernobyl. Environ. Pollut. 255, 113238 https://doi.org/10.1016/j.envpol.2019.113238.

Peeters, C., De Canck, E., Cnockaert, M., De Brandt, E., Snauwaert, C., Verheyde, B., Depoorter, E., Spilker, T., LiPuma, J.J., Vandamme, P., 2019. Comparative genomics of *Pandoraea*, a genus enriched in xenobiotic biodegradation and metabolism. Front. Microbiol. 10, 2556. https://doi.org/10.3389/fmicb.2019.02556.

Prendergast-Miller, M.T., de Menezes, A.B., Macdonald, L.M., Toscas, P., Bissett, A., Baker, G., Farrell, M., Richardson, A.E., Wark, T., Thrall, P.H., 2017. Wildfire impact: natural experiment reveals differential short-term changes in soil microbial communities. Soil Biol. Biochem. 109, 1–13. https://doi.org/10.1016/j.soilbio.2017.01.027.

Quast, C., Pruesse, E., Yilmaz, P., Gerken, J., Schweer, T., Yarza, P., Peplies, J., Glöckner, F.O., 2012. The SILVA ribosomal RNA gene database project: improved data processing and web-based tools. Nucleic Acids Res. 41, D590–D596. https://doi.org/10.1093/nar/gks1219.

Roehr, J.T., Dieterich, C., Reinert, K., 2017. Flexbar 3.0 - SIMD and multicore parallelization. Bioinforma. Oxf. Engl. 33, 2941–2942. https://doi.org/10.1093/bioinformatics/btx330.

Rosen, M.J., Callahan, B.J., Fisher, D.S., Holmes, S.P., 2013. Denoising PCR-amplified metagenome data. BMC Bioinformatics 13, 1–16. https://doi.org/10.1186/1471-2105-13-283.

Sharma, A., Gaidamakova, E.K., Grichenko, O., Matrosova, V.Y., Hoeke, V., Klimenkova, P., Conze, I.H., Volpe, R.P., Tkavc, R., Gostinčar, C., Gunde-Cimerman, N., DiRuggiero, J., Shuryak, I., Ozarowski, A., Hoffman, B.M., Daly, M.J., 2017. Across the tree of life, radiation resistance is governed by antioxidant $Mn^{2+}$, gauged by paramagnetic resonance. Proc. Natl. Acad. Sci. 114, E9253–E9260. doi:https://doi.org/10.1073/pnas.1713608114.

Sheremet, A., Jones, G.M., Jarett, J., Bowers, R.M., Bedard, I., Culham, C., Eloe-Fadrosh, E.A., Ivanova, N., Malmstrom, R.R., Grasby, S.E., Woyke, T., Dunfield, P.F., 2020. Ecological and genomic analyses of candidate phylum WPS-2 bacteria in an unvegetated soil. Environ. Microbiol. 22, 3143–3157. https://doi.org/10.1111/1462-2920.15054.

Shuryak, I., 2019. Review of microbial resistance to chronic ionizing radiation exposure under environmental conditions. J. Environ. Radioact. 196, 50–63. https://doi.org/10.1016/j.jenvrad.2018.10.012S.

Singh, H., 2018. Desiccation and radiation stress tolerance in cyanobacteria. J. Basic Microbiol. 58, 813–826. https://doi.org/10.1002/jobm.201800216.

Stark, K., Goméz-Ros, J.M., Vives i Batlle, J., Lindbo Hansen, E., Beaugelin-Seiller, K., Kapustka, L.A., Wood, M.D., Bradshaw, C., Real, A., McGuire, C., Hinton, T.G., 2017. Dose assessment in environmental radiological protection: state of the art and perspectives. J. Environ. Radioact. 175–176, 105–114. https://doi.org/10.1016/j.jenvrad.2017.05.001.

Stibal, M., Schostag, M., Cameron, K.A., Hansen, L.H., Chandler, D.M., Wadham, J.L., Jacobsen, C.S., 2015. Different bulk and active bacterial communities in cryoconite from the margin and interior of the Greenland ice sheet. Environ. Microbiol. Rep. 7, 293–300. https://doi.org/10.1111/1758-2229.12246.

Storey, J.D., 2002. A direct approach to false discovery rates. J. R. Stat. Soc. Ser. B Stat. Methodol. 64, 479–498.

Storey, S., Ashaari, M.M., Clipson, N., Doyle, E., de Menezes, A.B., 2018. Opportunistic bacteria dominate the soil microbiome response to phenanthrene in a microcosm-based study. Front. Microbiol. 9, 1–13. https://doi.org/10.3389/fmicb.2018.02815.

Theodorakopoulos, N., Février, L., Barakat, M., Ortet, P., Christen, R., Piette, L., Levchuk, S., Beaugelin-Seiller, K., Sergeant, C., Berthomieu, C., Chapon, V., 2017. Soil prokaryotic communities in Chernobyl waste disposal trench T22 are modulated by organic matter and radionuclide contamination. FEMS Microbiol. Ecol. 93, 1–12. https://doi.org/10.1093/femsec/fix079.

Videvall, E., Burraco, P., Orizaola, G., 2022. Impact of ionizing radiation on the environmental microbiomes of Chernobyl wetlands. bioRxiv. https://doi.org/10.1101/2022.01.17.476627.

Vives I Batlle, J., Balonov, M., Beaugelin-Seiller, K., Beresford, N.A., Brown, J., Cheng, J. J., Copplestone, D., Doi, M., Filistovic, V., Golikov, V., Horyna, J., Hosseini, A., Howard, B.J., Jones, S.R., Kamboj, S., Kryshev, A., Nedveckaite, T., Olyslaegers, G., Pröhl, G., Sazykina, T., Ulanovsky, A., Vives Lynch, S., Yankovich, T., Yu, C., 2007. Inter-comparison of absorbed dose rates for non-human biota. Radiat. Environ. Biophys. 46, 349–373. https://doi.org/10.1007/s00411-007-0124-1.

Vives I Batlle, J., Beaugelin-Seiller, K., Beresford, N.A., Copplestone, D., Horyna, J., Hosseini, A., Johansen, M., Kamboj, S., Keum, D.K., Kurosawa, N., Newsome, L., Olyslaegers, G., Vandenhove, H., Ryufuku, S., Vives Lynch, S., Wood, M.D., Yu, C., 2011. The estimation of absorbed dose rates for non-human biota: an extended intercomparison. Radiat. Environ. Biophys. 50, 231–251. https://doi.org/10.1007/s00411-010-0346-5.

Volkova, P.Y., Geras'Kin, S.A., Kazakova, E.A., 2017. Radiation exposure in the remote period after the Chernobyl accident caused oxidative stress and genetic effects in Scots pine populations. Sci. Rep. 7, 1–9. https://doi.org/10.1038/srep43009.

Wang, J., Wang, C., Li, J., Bai, P., Li, Q., Shen, M., Li, R., Li, T., Zhao, J., 2018. Comparative genomics of degradative *Novosphingobium* strains with special reference to microcystin-degrading *Novosphingobium* sp. THN1. Front. Microbiol. 9, 2238. https://doi.org/10.3389/fmicb.2018.02238.

Wintenberg, M., Manglass, L., Martinez, N.E., Blenner, M., 2023. Global transcriptional response of *Escherichia coli* exposed in situ to different low-dose ionizing radiation sources. mSystems 8, e00718-22. doi:https://doi.org/10.1128/msystems.00718-22.

Yamada, T., Sekiguchi, Y., 2009. Cultivation of uncultured Chloroflexi subphyla: significance and ecophysiology of formerly uncultured Chloroflexi "Subphylum I" with natural and biotechnological relevance. Microbes Environ. 24, 205–216. https://doi.org/10.1264/jsme2.ME09151S.

Zhao, J.K., Li, X.M., Ai, G.M., Deng, Y., Liu, S.J., Jiang, C.Y., 2016. Reconstruction of metabolic networks in a fluoranthene-degrading enrichments from polycyclic aromatic hydrocarbon polluted soil. J. Hazard. Mater. 318, 90–98. https://doi.org/10.1016/j.jhazmat.2016.06.055.